
# Coupled waves as a model to describe chaotic turbulence pumped by radio waves in the ionosphere

Axel Hahlin
*Author*

Thomas Leyser
*Supervisor*

Jan Bergman
*Subject Reader*

July 20, 2018

**Abstract**

Experimental results concerning plasma turbulence pumped in the ionosphere by powerful radio waves suggest that the turbulence is due to deterministic chaos. To investigate the possibility of deterministic chaos in the ionosphere coupled wave systems have been studied to see chaotic dynamics. If coupled waves can exhibit chaos it is a possible way to model ionospheric chaos. The result showed that chaos was present in both wave systems studied which means that they could possibly explain the chaos, to verify this more studies needs to be done on the parameters relevant to the coupled wave systems in the ionosphere and find if they are in a regime where chaos develops.

**Sammanfattning**

Studier av plasmaturbulens i jonosfären som pumpas av kraftfulla radiovågor antyder att turbulensen är kopplat till deterministiskt kaos. För att undersöka möjligheten för deterministiskt kaos i jonosfären studeras kopplade vågsystem om de kan innehålla kaotiska regimer. Om dessa system visar kaotiskt beteende skulle de kunna användas för att beskriva kaos i jonosfären. Resultatet visade att kaos var närvarande i de kopplade vågsystem som studerats, för att verifiera om de kan användas för att beskriva kaos i jonosfären måste närmare studier av de parametrar som modellen använder sig av göras för att se om de faller inom ett intervall där kaos uppstår.

# Contents


**1 Background** **4**
- 1.1 Ionospheric plasma . . . . . 4
- 1.2 EISCAT - European Incoheren SCATter association . . . . . 4
- 1.3 Deterministic Chaos . . . . . 4

**2 Turbulent flow** **5**
- 2.1 Origin of the flow potential . . . . . 5
- 2.2 Solution to the system . . . . . 6
  - 2.2.1 Closed Orbits . . . . . 7
  - 2.2.2 Separatrix . . . . . 8
- 2.3 Relation between the separatrix and Chaos . . . . . 9

**3 Three-wave coupling** **11**
- 3.1 Threshold for instability with wave damping . . . . . 11
- 3.2 Threshold for instability with frequency mismatch . . . . . 12
- 3.3 Combined threshold . . . . . 12
- 3.4 Turbulence in the three-wave system . . . . . 13

**4 Four-Wave coupling** **17**
- 4.1 Chaos with identical damping . . . . . 18
- 4.2 Chaos with strong coupling . . . . . 19
- 4.3 Chaos with multiple growing waves . . . . . 20

**5 Discussion** **21**

**6 Summary** **21**

**References** **22**

# 1 Background

## 1.1 Ionospheric plasma

The ionosphere starts at an altitude of 60km and reaches up to about 1000km[1]. In the ionosphere atoms and molecules will get ionised by solar radiation creating a plasma, as the altitude increases so does the proportion of ionised particles. Even if a plasma has a net neutral charge the electrons and heavier ions move differently when exposed to an electric field. This can create local areas with net charge. The approximate frequency at which the electron perturbations oscillate is given by the plasma frequency that is dependent on the density of the plasma. The electron plasma frequency is much higher than that of wave motions involving ion dynamics. In the report a waves in the plasma will be important. They will be defined with an angular frequency $\omega$ and the wavevector $\mathbf{k}$, these parameters will be used to couple the waves when discussing coupled nonlinear wave systems.[2]

## 1.2 EISCAT - European Incoheren SCATter association

The EISCAT-heating is a powerful high frequency transmitter of electromagnetic waves near Tromsø in Norway that sends strong monochromatic radio waves that pumps energy into the ionosphere. This energy feeds into a wide range of different plasma waves inside the ionosphere. The experiments done show that the pumped plasma turbulence emits a rich spectrum of electromagnetic waves at different frequencies [3]. In particular, the results in figure 2 show that the frequency spectra are exponential. Exponential spectra have been associated with deterministic chaos involving pulses with a Lorentzian form.

## 1.3 Deterministic Chaos

The central part of this report studies the notion of deterministic chaos, which is a dynamic that during certain conditions can occur in a nonlinear system where the result is dependent on initial conditions. Note that this form of chaos is not random but deterministic so the result will always be the same for identical initial conditions. Of particular interest in this report is to study models of nonlinear wave interactions which may exhibit chaotic behaviour and could be related to turbulence observed in the ionosphere. A model that is of particular interest is a system of four coupled waves where one wave is resonant with the pump wave, the reason for this is that it allows waves with a higher frequency than the pump wave to be created compared to a more simple three-wave system. The particular four wave system to be studied can be considered a double three-wave system, in which two of the waves are shared between the two wave triplets.

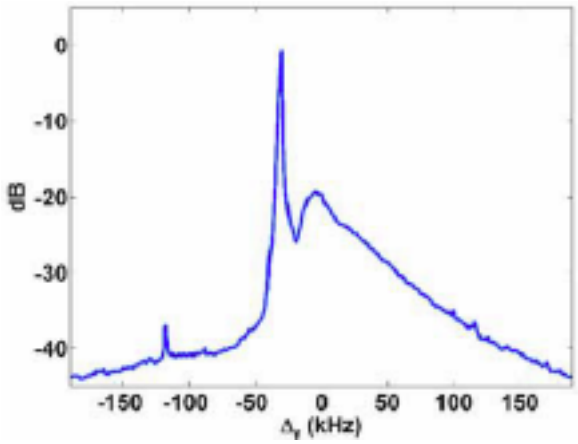


Figure 2: Experimental results showing the frequencies observed with frequencies compared to the radio wave used to pump the waves inside the plasma. The ionospherically reflected pump wave is the strong peak at -30kHz. The spectral feature that is up-shifted from the pump frequency is emitted by the stimulated plasma turbulence. Provided by Thomas Leyser.

# 2 Turbulent flow

Since the chaotic behaviour is connected to Lorentzian pulses the ionised atoms should flow such that Lorentzian pulses are present. It is therefore interesting to see how the particles flows inside the plasma when affected by electromagnetic fields and if this flow could show chaotic behaviour. This will be done by studying a flow potential given by Maggs and Morales [4] that has Lorentzian characteristics in the flow lines.

## 2.1 Origin of the flow potential

Before the flow potential is introduced a quick derivation of how the flow potential causes motion in a plasma. Here the Lorentz force is acting on the plasma,

$$\mathbf{F} = q(\mathbf{E} + \mathbf{v} \times \mathbf{B}) \tag{1}$$

In equilibrium $\mathbf{F} = 0$, which gives:

$$-\mathbf{E} = \mathbf{v} \times \mathbf{B} \tag{2}$$

The magnetic field in question is the earth's magnetic field, which is assumed to be constant. This means that:

$$\nabla \times \mathbf{E} = -\frac{\partial \mathbf{B}}{\partial t} = 0$$

So $\mathbf{E}$ can be expressed as a gradient of a scalar potential $\Phi$.

$$\mathbf{E} = -\nabla\Phi$$

Substituting this into equation (2) gives:

$$\nabla\Phi = \mathbf{v} \times \mathbf{B}$$

Expanding the expression by $\mathbf{B}\times$ on each sides gives:

$$\mathbf{B} \times \nabla\Phi = \mathbf{B} \times \mathbf{v} \times \mathbf{B}$$

Vector identities simplify the right hand side to:

$$\mathbf{B} \times \nabla\Phi = \mathbf{v}(\mathbf{B} \cdot \mathbf{B}) - \mathbf{B}(\mathbf{B} \cdot \mathbf{v})$$

Here $\mathbf{v}$ and $\mathbf{B}$ are perpendicular, which gives:

$$\mathbf{B} \times \nabla\Phi = B^2\mathbf{v}$$

This expression can be solved for $\mathbf{v}$:

$$\mathbf{v} = \frac{1}{B^2}\mathbf{B} \times \nabla\Phi$$

where $\mathbf{B}/B = \hat{\mathbf{z}}$ finally yields:

$$\mathbf{v} = \frac{1}{B}\hat{\mathbf{z}} \times \nabla\Phi \tag{3}$$

It is interesting to study a potential that gives Lorentzian motion, such a potential is given by Maggs and Morales [4]:

$$\Phi(x, y) = -(x^2 + c^2)y^2 + by \tag{4}$$

From equation (3) the velocity field for the potential (4) is obtained:

$$\begin{aligned} v_x &= 2y(x^2 + c^2) - b \\ v_y &= -2xy^2 \end{aligned} \tag{5}$$

The field has a single stationary point where $v_x = v_y = 0$. This occurs at the point $x = 0$ and $y = b/2c^2$.

## 2.2 Solution to the system

The potential in equation (4) has been studied and discussed by Maggs and Morales [4]. They considered the flow lines from equation (5) that are solved for constant $\Phi$. This results in three different families of solutions, distinguished by the value of $\Phi$.

$$\Phi \begin{cases} > 0, & \text{closed orbits} \\ = 0, & \text{separatrix} \\ < 0, & \text{unbounded orbits} \end{cases}$$

Of particular interest are the closed orbits and the separatrix that is the border between the closed and unbounded trajectories.

### 2.2.1 Closed Orbits

The system of equations (5) for $\Phi > 0$ has the solution:

$$y(t) = \frac{2\Phi_0/b}{1 + \sqrt{1 - 4c^2\Phi_0/b^2}\cos(2\sqrt{\Phi_0}t)} \tag{6}$$

Expanding (6) yields:

$$y(t) = \frac{b}{2c^2}\frac{4c^2\Phi_0/b^2}{1 + \sqrt{1 - 4c^2\Phi_0/b^2}\cos(2\sqrt{\Phi_0}t)}$$

Miloh and Tulin [5] showed that is possible to express $\delta^2/(1 + \sqrt{1-\delta^2}\cos(\omega t))$ as an infinite series of Lorentzian pulses with equal amplitude and temporal spacing.

$$\frac{\delta^2}{1 + \sqrt{1 - \delta^2}\cos(\omega t)} = k\sum_{n=-\infty}^{\infty}\frac{1}{1 + (t - n2\pi/\omega)^2/\gamma^2} \tag{7}$$

Where

$$k = 2\delta/\tanh^{-1}\delta \qquad \gamma = (1/\omega)\tanh^{-1}(\delta)$$

For the solution given in equation (6) $\delta = 2c\sqrt{\Phi_0}/b$. Replacing $k$ and $\gamma$ in the right-hand side of equation (7):

$$\frac{4c\sqrt{\Phi_0}}{b\tanh^{-1}(2c\sqrt{\Phi_0}/b)}\sum_{n=-\infty}^{\infty}\frac{1}{1 + \left((t - 2n\pi/\omega)\omega/(\tanh^{-1}(2c\sqrt{\Phi_0}/b)\right)^2}$$

This gives an expression for $y(t)$:

$$y(t) = \frac{2\sqrt{\Phi_0}}{c\tanh^{-1}(2c\sqrt{\Phi_0}/b)}\sum_{n=-\infty}^{\infty}\frac{1}{1 + \left((t - 2n\pi/\omega)\omega/(\tanh^{-1}(2c\sqrt{\Phi_0}/b)\right)^2}$$

From equation (6) $\omega = 2\sqrt{\Phi}$:

$$y(t) = \frac{2\sqrt{\Phi_0}}{c\tanh^{-1}(2c\sqrt{\Phi_0}/b)}\sum_{n=-\infty}^{\infty}\frac{1}{1 + \left((t - n\pi/\sqrt{\Phi_0})2\sqrt{\Phi_0}/(\tanh^{-1}(2c\sqrt{\Phi_0}/b)\right)^2}$$

The expression inside the sum is a Lorentzian pulse of amplitude 1 and width $\tau = \tanh^{-1}(2c\sqrt{\Phi_0}/b)/(2\sqrt{\Phi_0})$. The sum also results in a time separation between two consecutive pulses of $\pi/\sqrt{\Phi_0}$. The expression can finally be written as:

$$y(t) = \frac{1}{c\tau}\sum_{n=-\infty}^{\infty}\frac{1}{1 + \left((t - n\pi/\sqrt{\Phi_0})/\tau\right)^2} \tag{8}$$

This is the same equation obtained in Maggs and Morales [4]. In equation (8) the amplitude of the Lorentzian pulses is given by $1/(c\tau)$.

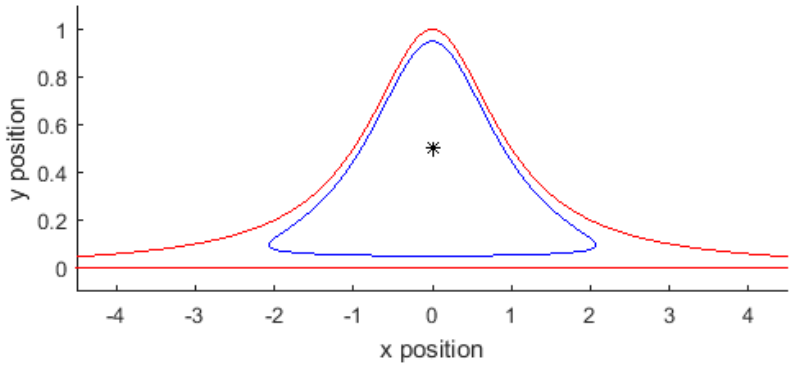


Figure 3: The separatrix (red) and the flow line for a closed orbit for $\Phi = 0.0474$ (blue).

### 2.2.2 Separatrix

The separatrix is the group of solutions where the flow potential (equation (4)) has the constant value $\Phi = 0$. Solving the system gives trajectories of the form:

$$y(t) = \frac{b/c^2}{1 + b^2t^2/c^2}, \qquad x(t) = bt \tag{9}$$

The behaviour of trajectories are very dependent on which side of the separatrix they are on. Particularly trajectories close to the separatrix could change behaviour if a small perturbation is introduced to the system, this is possibly connected to the chaotic behaviour of the system when parameters are modulated.

## 2.3 Relation between the separatrix and Chaos

Maggs and Morales [4] showed in a simulation that the system (5) exhibits chaotic behaviour when the parameter $b$ is periodically modulated. The modulation is done by adding a trigonometric term with a frequency that is scaled to the frequency $f_s = \frac{1}{2\pi}$, so that $b$ oscillates sinusoidally in the range $0.5 < b < 1.5$.

This simulation was repeated using the fourth order Runge-Kutta method and the same initial conditions used by Maggs and Morales, it was done for modulation frequencies in the range $[0, 1.05] * f_s$. The result of this simulation can be seen in figure (4). The figure shows the sequence for a certain value of the modulation frequency where the colours indicate the $y$-amplitude in the flow potential. For certain values of $f$ the amplitude show a very varying behaviour for small changes of $f$ which is an indication of chaos.

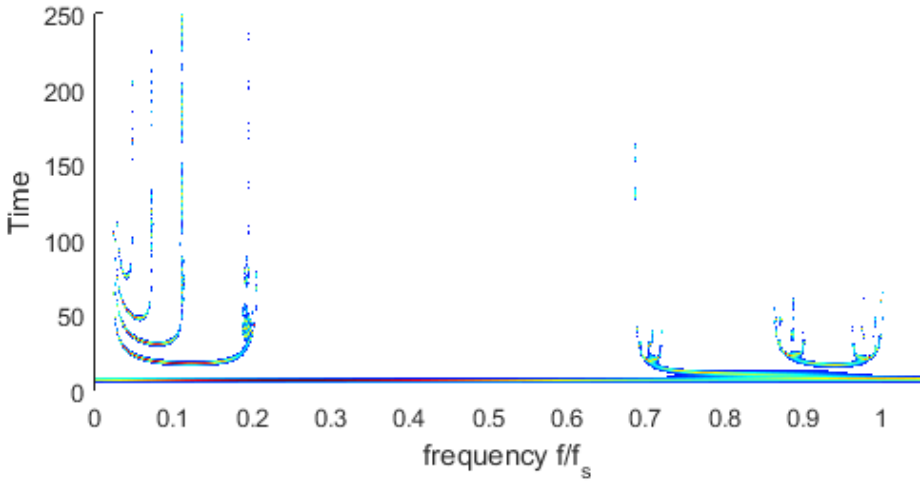


Figure 4: Shown in figure is the $y$-amplitude of a particle inside the flow potential for different modulation frequencies $f$, scaled over $f_s = \frac{1}{2\pi}$.

This turbulence was proposed by Maggs and Morales to come from trajectories close to the separatrix changing topological behaviour when the trajectories cross the separatrix as $b$ is modulated. To verify this claim the amplitude of the trajectory was compared to the separatrix in the simulation and whenever the difference between the two values changed sign a crossing was recorded and plotted in figure (5). Figure (6) show both previous figures combined to more readily compare the separatrix crossings with the intervals of chaotic behaviour.

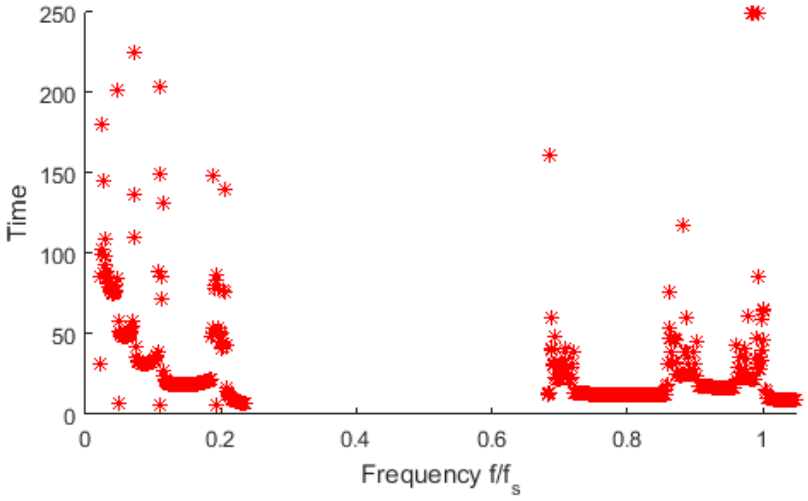


Figure 5: Shown are the occasions when the moving particle, for a certain modulation frequency $f$, changed topological behaviour by crossing the separatrix (equation (9)).

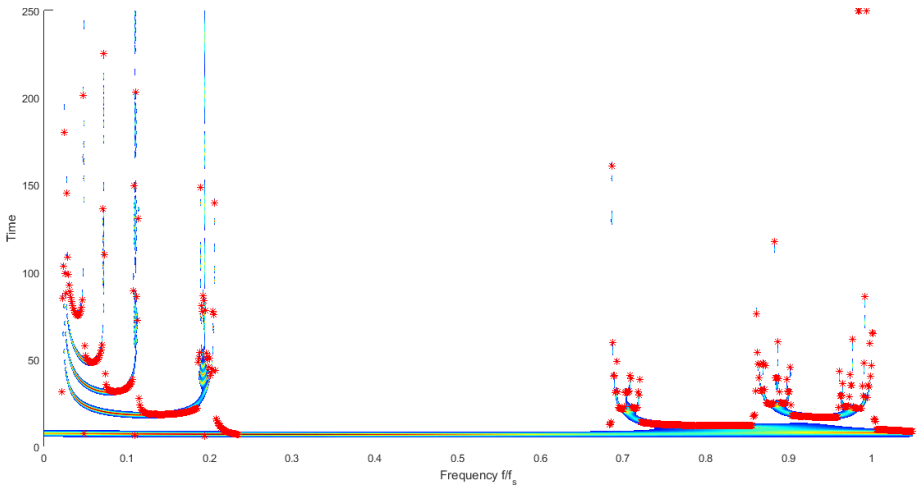


Figure 6: Figures (4) and (5) placed on top of each other to compare the chaotic regions with the separatrix crossings.

It can be seen from figure (6) that the regions where the trajectories crosses the separatrix closely correspond to the areas where chaotic behaviour is present. This shows that the topological change coming from the proximity of the separatrix could be one of the underlying reasons behind the observed chaos.

# 3 Three-wave coupling

The interactions that will be studied in the following chapter is three coupled waves satisfying the conditions $\omega_1 \approx \omega_2 + \omega_3$ and $\mathbf{k}_1 = \mathbf{k}_2 + \mathbf{k}_3$, following Lopes and Chian [6]. Such three-wave interaction may be an important part of the observed turbulent behaviour in the ionosphere. In particular the regimes where the system shows an unstable behaviour is of interest since this is where chaotic dynamics becomes possible. The system of three-wave coupling that will be studied in this section is seen below,

$$\begin{cases} \dot{A}_1 = \nu_1 A_1 + A_2 A_3 \\ \dot{A}_2 = i\delta A_2 + \nu_2 A_2 - A_1 A_3^* \\ \dot{A}_3 = \nu_3 A_3 - A_1 A_2^* \end{cases} \tag{10}$$

Here $A_j$ is the amplitude of each wave and $\nu_j$ is a damping factor of the wave. Finally $\delta$ is a frequency mismatch of the form $\delta = (\omega_1 - \omega_2 - \omega_3)/\chi$. For such normalisation the time derivative is with respect to the characteristic time $\tau = \chi t$ with $\chi$ as the characteristic frequency. First the threshold for instability in the initial moment of the system will be studied. The threshold will show how strong the pump wave must be to overcome various damping effects of the system. This is important since if the pump wave is not strong enough to overcome this threshold no chaos will occur in the system.

## 3.1 Threshold for instability with wave damping

In order to study the system some simplifications will be done. First the amplitudes are assumed to be real valued ,the frequency shift $\delta$ is assumed to be zero and the amplitude of the pump wave is$A_1 >> A_2, A_3$ initially. If the amplitudes $A_2$ and $A_3$ start of small the non-linear terms will be approximately zero for a short duration after the initial state. In addition the amplitude for the first wave is assumed to be constant while $\nu_2 = \nu_3 = \nu$. With these assumptions the system (10) simplifies to,

$$\begin{cases} \dot{A}_2 = -\nu A_2 - A_1 A_3 \\ \dot{A}_3 = -\nu A_3 - A_1 A_2 \end{cases} \tag{11}$$

or in matrix notation.

$$\begin{bmatrix} \dot{A}_2 \\ \dot{A}_3 \end{bmatrix} = \begin{bmatrix} -\nu & -A_1 \\ -A_1 & -\nu \end{bmatrix} \begin{bmatrix} A_2 \\ A_3 \end{bmatrix}$$

If exponential solutions of the form $ce^{\lambda\tau}$ are assumed, $\lambda$ will take the values of the eigenvalues of the matrix $M$ from equation (11). These eigenvalues can be found from $det(M - \lambda\mathbb{I}) = 0$.

$$det \begin{bmatrix} -(\nu + \lambda) & -A_1 \\ -A_1 & -(\nu + \lambda) \end{bmatrix} = 0$$

$$(\nu + \lambda)^2 - A_1^2 = 0$$

Solving this for $\lambda$ gives:

$$\lambda = -\nu \pm A_1 \tag{12}$$

For the system to exhibit unstable behaviour, the obtained eigenvalue must be positive which only holds when $A_1 > \nu$. This results shows that the amplitude of $A_1$ must be greater than the damping coefficient of waves 2 and 3 for instability.

## 3.2 Threshold for instability with frequency mismatch

The second interesting case is when there is no damping but the frequencies have a small shift such that $\omega_1 \approx \omega_2 + \omega_3$. In other words $\nu_j = 0$ but $\delta \neq 0$. As in the previous example we are interested to investigate the possibility of instability, which means that only the first moment will be studied. In this time interval both $A_2$ and $A_3$ will be significantly smaller than $A_1$ which can be assumed to be constant. This simplifies system (10) to,

$$\begin{cases} \dot{A}_2 = i\delta A_2 - A_1 A_3^* \\ \dot{A}_3 = -A_1 A_2^* \end{cases} \tag{13}$$

To solve this we differentiate the first equation in the system with respect to time and obtain

$$\ddot{A}_2 = i\delta \dot{A}_2 - A_1 \dot{A}_3^*$$

Here $\dot{A}_3$ can be replaced with the expression in system (13).

$$\ddot{A}_2 = i\delta \dot{A}_2 + A_1^2 A_2$$

This is a second order linear equation that can be solved with the assumption that $A_2 = a_2 e^{b_2 t}$. The values obtained for $b_2$ is

$$b_2 = i\frac{\delta}{2} \pm \sqrt{A_1^2 - \frac{\delta^2}{4}} \tag{14}$$

This solutions shows instability when $b_2$ has a nonzero real value, this happens when $|A_1| > |\frac{\delta}{2}|$. This means that instability appears when the amplitude is larger than half of the frequency mismatch. Higher amplitudes will cause a larger interval in which coupled three-wave systems are unstable.

## 3.3 Combined threshold

In reality, however, a system will have both damping and a frequency mismatch. The pump wave $A_1$ is still assumed to be constant and the question is what threshold $A_1$ has to exceed to make the system unstable. With the experience from the previous sections similar computations can be done. Equation (10) with $A_1$ constant becomes

$$\begin{bmatrix} \dot{A}_2 \\ \dot{A}_3 \end{bmatrix} = \begin{bmatrix} i\delta - \nu & -A_1 \\ -A_1 & -\nu \end{bmatrix} \begin{bmatrix} A_2 \\ A_3 \end{bmatrix} \tag{15}$$

The eigenvalues of this matrix can be determined,

$$det \begin{bmatrix} i\delta - \nu - \lambda & -A_1 \\ -A_1 & -\nu - \lambda \end{bmatrix} = 0$$

Solving this yields,

$$\lambda = \frac{i\delta}{2} - \nu \pm \sqrt{A_1^2 - \frac{\delta^2}{4}}$$

Once again the real valued part of $\lambda$ must be positive, which occurs when

$$|A_1| > |\frac{\delta}{2}|, \qquad \nu < \sqrt{A_1^2 - \frac{\delta^2}{4}}$$

From this the threshold for $A_1$ is obtained to be,

$$|A_1| > \sqrt{\nu^2 + \frac{\delta^2}{4}} \tag{16}$$

Compared to the previous two cases it can be seen that the threshold is higher since both $\nu$ and $\delta$ contributes to the threshold. It can also be seen that equation (16) reduces to the simpler cases studied earlier in the chapter when $\nu$ or $\delta = 0$.

To verify this threshold numerically $\nu$ and $\delta$ are chosen arbitrary, the initial amplitudes of the waves are chosen such that $A_1 >> A_2, A_3$ and the value of $A_1$ is in close proximity of the threshold obtained in equation (16). System (15) is then numerically integrated over a time interval to see if it approaches zero or grows exponentially. Results from two different starting values of $A_1$ close to the computed threshold can be seen in figure 7. It can be seen that for values higher than the threshold the amplitudes grow while damping is observed for values lower than the required threshold.

## 3.4 Turbulence in the three-wave system

So far the system has either been growing exponentially or has been damped and unable to develop any turbulent behaviour. To see if a three-wave system can become turbulent some simplification done earlier in the chapter must be removed, this requires a numerical analysis.

In the numerical study of system (10) the wave $A_1$, which previously was assumed to be constant, is instead assumed to be growing with $\nu_1 > 0$ while $A_2$ and $A_3$ are still damped with $\nu_2 = \nu_3 = -\nu < 0$. The system is then numerically integrated for a certain value of the frequency miss match $\delta$ and for various values of $\nu$. The numerical solution in figure 8 shows the amplitudes of local maximums of $|A_2|$ in a time interval after the system has had time to stabilise. At low values of $\nu$ the system has only one amplitude but when $\nu$ reaches a certain value the amplitude bifurcates into two branches, which is called period doubling by Chian et al [7]. The period doubling means that the system changes its behaviour such that it has double the period compared to the previous behaviour. This repeats until the system shows an almost continuous

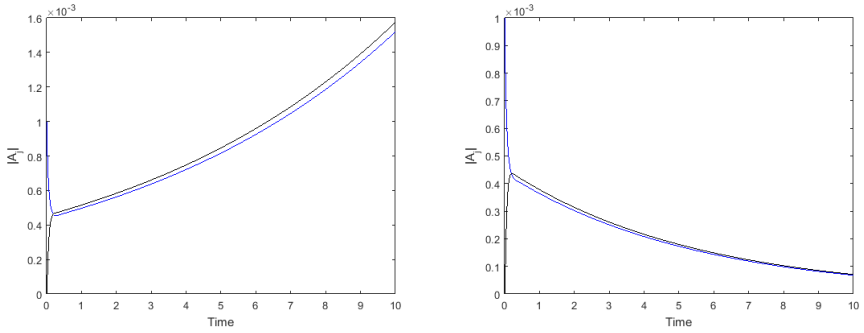


(a) Time evolution for system (15) with $A_1$ = computed threshold +0.3

(b) Time evolution for system (15) with $A_1$ =computed threshold +0.0

Figure 7: The amplitudes of $A_2$(blue) and $A_3$(black) for $A_1$ amplitudes close to the threshold computed in equation 16. For values above the threshold the system begins to grow while a damping is observed for values at or below the threshold.

range of possible amplitudes at higher $\nu$. Previously it was mentioned that deterministic chaos is associated with exponential power spectra. This can be tested by Fourier transform on the amplitude for the wave $A_2$. In figure 9 it can be seen that the system exhibits exponential frequency spectra for a range of frequencies. Comparing the results from the figures 9a and 9b $\nu = 16$ shows exponential behaviour for a larger range. From figure 8a it can be seen that $\nu = 16.0$ is in a region with more possible amplitudes compared with $\nu = 13.6$.

Comparing the effects of different $\delta$ it can be seen from figure 8 that the period doubling sets in at lower $\nu$ for higher $\delta$. To see how the system approach the period doubling the amplitude of $A_1$ is shown in figure 10 for three different $\nu$. At these values figure 8 shows that the amplitude should obtain one value, the system has only one stable frequency. What is seen in the image is that the peaks converges both from below and above but that the convergence is slower for higher values of $\nu$. The period doubling thus occurs as the convergence time tends to infinity. This means that there are two stable amplitude peaks instead of one and that the new frequency has twice the period as the original one. Figure 11 shows a similar behaviour where the value of $\delta$ has been varied close to the first bifurcation point in figure 8.

As $\nu$ increases the system exhibits a higher chaotic behaviour. To see how the system reacts to a change of $\delta$ the system is solved numerically for a variety of $\delta$ and the results can be seen in figure 12. The clear difference compared to the variation of $\nu$ is that as $\nu$ grow the period doubling continue and the system show an increasing number of possible amplitudes. For $\delta$ the period doubling only occurs for lower values, after a certain point the possible amplitudes begin to reduce. This indicate that for a system with a given damping $\nu$ there exists a specific interval of frequency shifts $\delta$ where chaotic behaviour is possible.

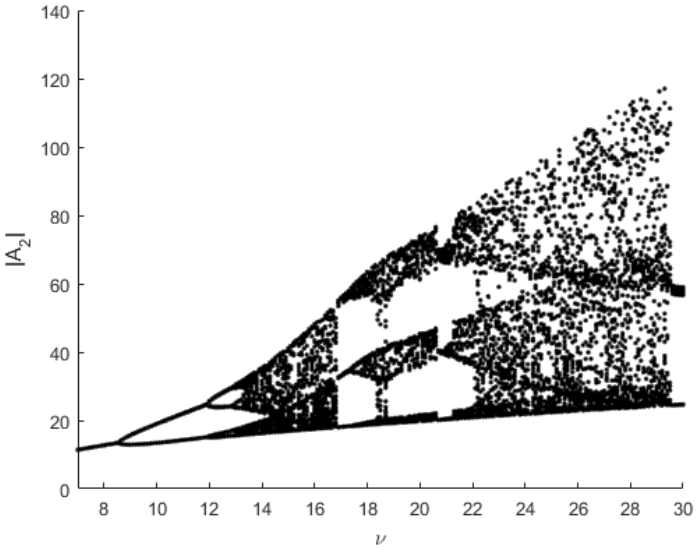


(a)

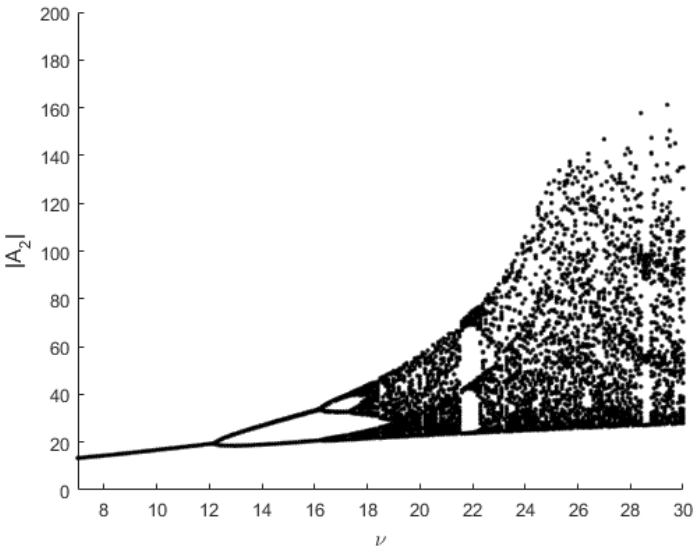


(b)

Figure 8: Each point shows a peak value of the amplitude $A_2$ obtained for various $\nu$ with $\delta = 2$ in 8a and $\delta = 0.5$ in 8b. Note that these amplitudes are obtained after the system has stabilised from the initial conditions.

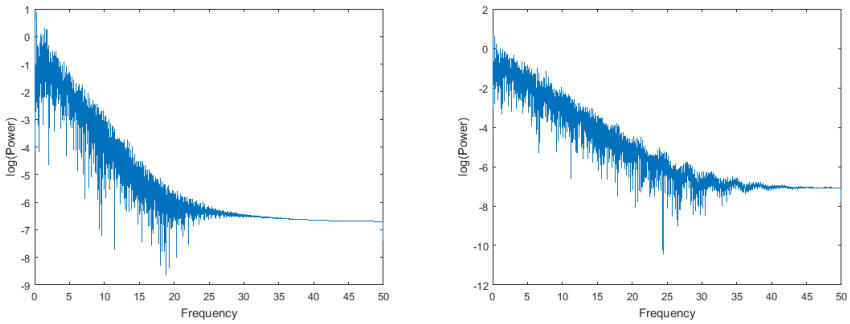


(a) $\nu = 13.6$ (b) $\nu = 16.0$

Figure 9: The Fourier transform for different $\nu$ of $|A_2|$ with $\delta = 2$

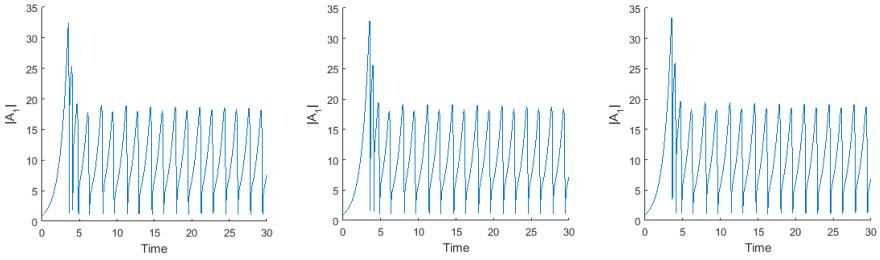


(a) $\nu = 8$ (b) $\nu = 8.1$ (c) $\nu = 8.2$

Figure 10: The amplitude of $A_1$ during the initial state of the system for slight variations in $\nu$.

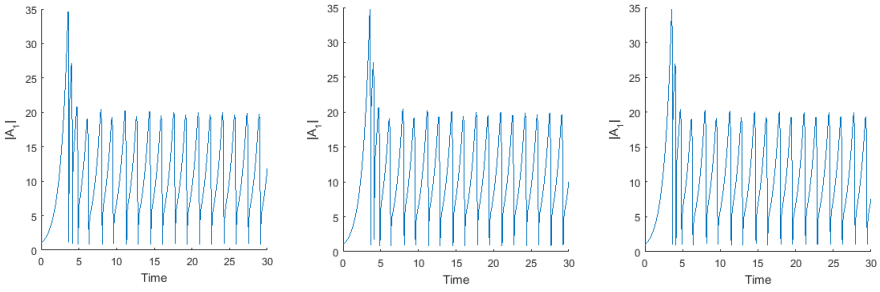


(a) $\delta = 1.5$ (b) $\delta = 1.6$ (c) $\delta = 1.8$

Figure 11: Similarly to figure 10 the amplitude of $A_1$ is shown for three different $\delta$ close to the bifurcation point.

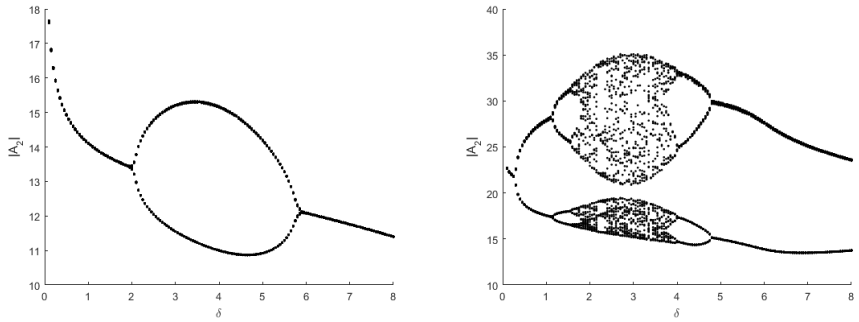


(a) $\nu = 8.5$ (b) $\nu = 13.6$

Figure 12: The amplitudes of $A_2$ is shown while $\nu$ is held constant and $\delta$ is varied over an interval

# 4 Four-Wave coupling

The next step is to introduce a fourth wave $A_4$ to the system. This comes in the form of two coupled three-wave systems where two of the waves are shared between both three-wave systems. The three-wave systems have conditions similar to the three-wave system studied in the previous chapter. The first system is identical to the system covered in chapter 3 with the conditions $\omega_1 \approx \omega_2 + \omega_3$ and $\mathbf{k}_1 = \mathbf{k}_2 + \mathbf{k}_3$. The second system includes the fourth wave with the conditions, $\omega_4 \approx \omega_1 + \omega_3$ and $\mathbf{k}_4 = \mathbf{k}_1 + \mathbf{k}_3$. Here $A_1$ is the plasma wave that is pumped by the radio waves sent into the ionosphere. The two three-wave systems combine into the following four-wave system obtained from Lopes and Chian [6], but modified to account for no wave being held constant and the different coupling strengths inside the system.

$$\begin{cases} \dot{A}_1 = \nu_1 A_1 + A_2 A_3 - r A_4 A_3^* \\ \dot{A}_2 = \nu_2 A_2 - A_1 A_3^* \\ \dot{A}_3 = i\delta_3 A_3 + \nu_3 A_3 - A_1 A_2^* - r A_4 A_1^* \\ \dot{A}_4 = i\delta_4 A_4 + \nu_4 A_4 + r A_1 A_3 \end{cases}$$

Since a second three wave system is introduced we define a coupling constant $r$ that shows the relative coupling strength in the two systems. Since $A_1$ is related to the pump wave it might be tempting to put it constant to simplify the system. There are however some issues with this, if $\dot{A}_1 = 0$ the system becomes linear and any possibilities for chaos disappears. Instead $A_1$ is a wave that is provided energy by the pump wave and is therefore assumed to be growing ($\nu > 0$). For the other waves a few different possibilities exists which will be studied in the chapter.

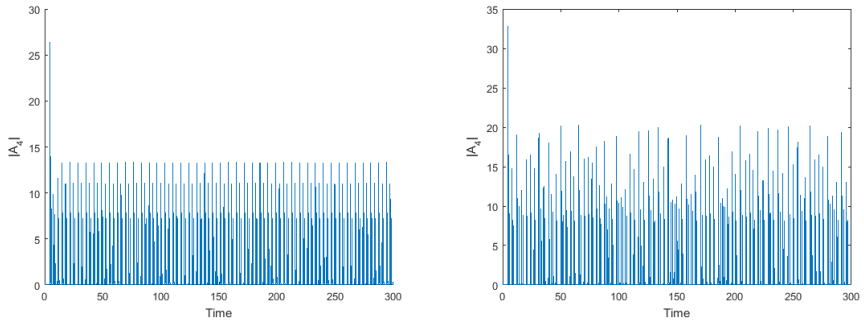


(a) $\nu = 11.5$ (b) $\nu = 14.0$

Figure 13: The time series for two different values of $\nu$ but for the same $\delta = 2$ and $r = 0.5$

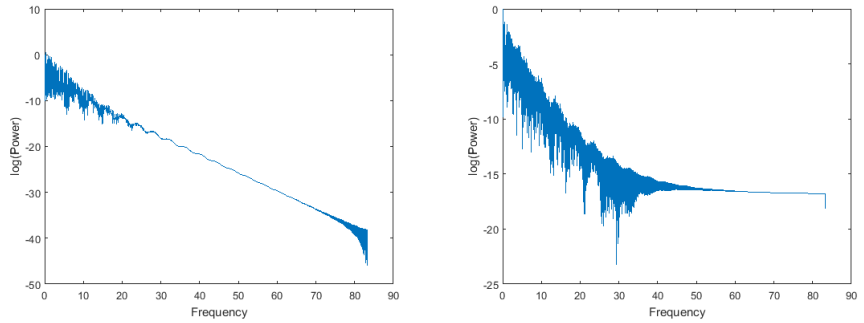


(a) $\nu = 11.5$ (b) $\nu = 14$

Figure 14: Fourier transforms of each time sequence from figure 13.

## 4.1 Chaos with identical damping

In this case all waves besides $A_1$ are assumed to be damped with $\nu_2 = \nu_3 = \nu_4 = -\nu$ while $\nu_1 = 1$. The frequency mismatches in the system are equal $\delta_3 = \delta_4$, here $\delta_3$ is the frequency mismatch from the first triplet and $\delta_4$ from the second triplet. The coupling coefficient of the second three-wave system is taken to be $r < 1$. To study the chaos the system is numerically integrated in a similar way to the three-wave system.

Figure 13 shows the time developments for the system at two different values $\nu$, in 13a chaos has not yet set in as the amplitude peaks of $A_4$ tends towards only three different values with a regular period. For 13b however the amplitude peaks take on a wide range of values and does so in an unpredictable way, thus the system exhibits chaos. The Fourier transforms in figure 14 show exponential power spectra, which can be associated with Lorentzian pulses.

To see how the system develops as the damping parameter $\nu$ is changed

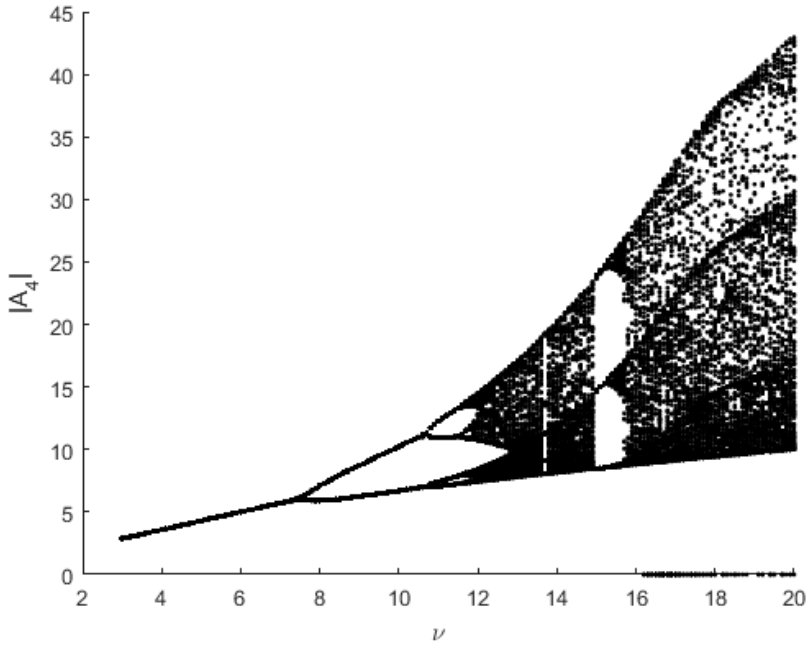


Figure 15: The development of the system when $\nu$ is changed while $\delta$ and $r$ are kept constant at 2 and 0.5 respectively.

the various amplitudes of $A_4$ after the system has moved sufficiently far from its initial conditions are plotted for different values $\nu$ and displayed in figure 15. This shows that as $\nu$ grows the system doubles the number of possible amplitudes at certain values of $\nu$ similarly to how the three-wave system behaved in figure 8. Here the regimes where deterministic chaos is present is where a large amount of amplitudes are possible for a single $\nu$. Comparison with the two time sequences in figure 13 it can be seen that $\nu = 11.5$ is in region with four periods for the amplitudes where two are very close to each other while $\nu = 14$ is in a regime where a large variety of amplitudes are possible.

## 4.2 Chaos with strong coupling

In the previous example the second wave triplet was considered to have a lower coupling strength compared to the first. Here all assumptions are the same as previous except for the fact that $r > 1$. When the system is run for the same parameters $\nu$, $\delta$ as before and $r = 5$ the system does not exhibit chaos but grows exponentially and eventually blows up. Even when $r$ is assumed to be connected to the first wave triplet and has a value $< 1$ the system grows exponentially. The conclusion is that the coupling strength of the second wave triplet cannot be significantly larger than the original triplet for chaos to occur.

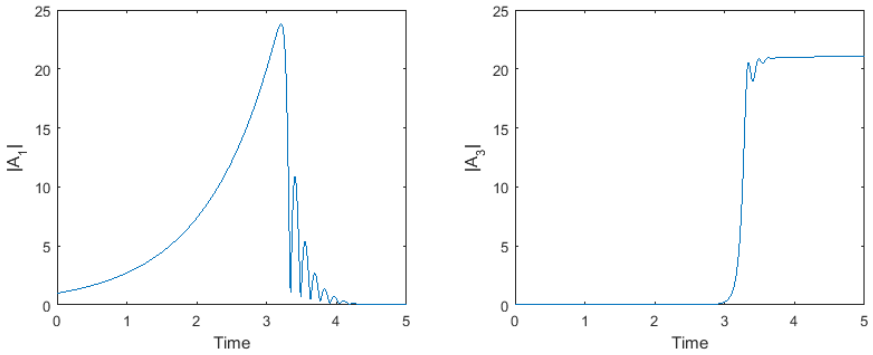


(a) $A_1$ (b) $A_3$

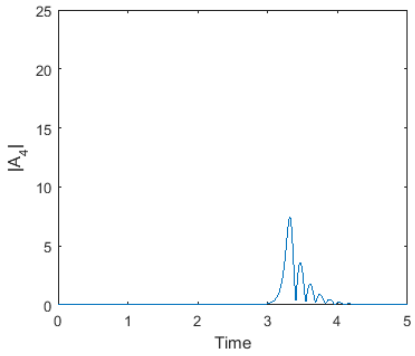


(c) $A_4$

Figure 16: Amplitudes for $A_1$, $A_3$ and $A_4$ in the beginning of the system, here $\nu_3 = 0.001\nu_1$, $\nu = 11.5$, $\delta = 2$ and $r = 0.5$.

This is consistent with that to excite waves with higher frequency than that of the pump wave if more difficult than to excite waves with lower frequencies.

### 4.3 Chaos with multiple growing waves

In the two prior examples all waves besides the wave that is provided with energy by the pump wave are considered to be damped. It might be possible that one of the other waves are also given energy from another source and grows on its own. This source is however assumed to be smaller compared to the pump wave that provides energy to $A_1$. As such $\nu_2 = \nu_4 = -\nu$, $\nu_1 = 1$ and $0 < \nu_3 < 1$ while the frequency mismatches are considered equal and $r < 1$. The result of allowing $A_3$ to grow is that as the other waves loses amplitude after the initial interaction $A_3$ continues to grow, eventually this also leads to exponential growth of the other waves in the system. The result is that if both $A_1$ and $A_3$ are allowed to grow it will eventually cause the entire system to grow exponentially and no

chaos will be present. If another wave is given energy from another source that source can not be allowed to exceed the damping of the surrounding plasma for an extended length of time.

# 5 Discussion

The study shows that chaotic regimes exists in a coupled four-wave system, which could make it a possible model to describe the turbulence observed in the ionosphere when it is pumped by strong radio waves. In addition certain parameter restrains for the existence of chaotic behaviour was discovered. The other waves in the system must not grow with energy provided by other sources and the wave triplet with the higher frequency wave must be more weakly coupled compared to the other triplet.

Since this study has been focused on the mathematical model the actual parameters in the ionosphere remains unknown. To test if this model is able to describe the chaotic behaviour observed, various parameters that was used in the models must be more closely determined by further study of the ionosphere. Should these parameters be found to coincide with a chaotic regime, the conclusion would be that ionospheric chaos is likely caused by wave interactions of the form studied here in this report. If not, other models must likely be explored to fully understand ionospheric chaos.

Both the three- and four-wave systems behave rather similarly and chaos occurs in both so why is the more complex four wave system of interest? This is because the fourth wave has a higher frequency compared to the pump wave. The observed data shows the presence of higher frequency waves which can not be reproduced by the three-wave system since both waves have a lower frequency compared to the pump wave.

# 6 Summary

Experimental results concerning plasma turbulence pumped by powerful radio waves in the ionosphere suggest that the turbulence is due to deterministic chaos. So far no model has explained the interactions that cause the observed turbulence. A possible model containing coupled waves has been studied to find regimes where the system exhibits chaos. This has been done analytically by making assumptions that simplify the systems, or numerically when a more exact treatment is needed. Chaos has been shown to exist in three- and four-wave systems, there is also a quite large regime where this chaos exists which indicates that the models does not require very specific condition to function. In particular, the coupled four-wave systems could explain the chaos observed in the ionosphere since the model includes a wave with up-shifted frequency similarly to what has previously been observed. To be certain however a closer study of the parameters in the model must be done to see if they are present in a chaotic regime in the ionosphere.

# References


[1] J. Law and R. Rennie. *A Dictionary of Physics (7 ed.)*. Oxford University Press, 2015.

[2] D.G. Swanson. *Plasma waves 2nd edition*. IOP publishing, 2003.

[3] T. B. Leyser. Stimulated electromagnetic emissions by high-frequency electromagnetic pumping of the ionospheric plasma. *Space Science Reviews*, 98:223–328, 2001.

[4] J.E. Maggs and G.J. Morales. Origin of lorentzian pulses in deterministic chaos. *Physical review, vol. 86, 015401*, 2012.

[5] T. Miloh and M.P. Tulim. Periodic solution of the dabo equation as a sum of repeated solitions. *Journal of Physics A: Mathematical and General, vol 22, 7*, 1989.

[6] S.R. Lopes and A.C.-L. Chian. Controlling chaos in nonlinear three-wave coupling. *Physical Review E, vol. 54(1):170-174*, 1996.

[7] A. Chian, J.R. Abalde, F.A. Borotto, S.R. Lopes, and F.B. Rizzato. Nonlinear dynamics and chaos in space plasmas. *Progress of Theoretical Physics Supplement*, (139):34–45, 2000.